International Journal of Engineering & Technology, 7 (4) (2018) 4563-4569

International Journal of Engineering & Technology

Website: www.sciencepubco.com/index.php/IJET
doi: 22669
Research paper

Numerical solution of the problem of spatially loaded rods in linear and geometrically nonlinear statements

Anarova Shahzoda Amanbayevna [1] *, Nuraliyev Faxriddin Murodillayevich [2], Usmonov Botir Shukurillayevich [3], Chulliyev Shohruh Ibodullayevich [4]

[1] *Doctor of Sciences Tashkent University of Information Technologies Named after Muhammad Al-Khwarizmi, Tashkent, Uzbekistan*
[2] *Doctor of Sciences Tashkent University of Information Technologies Named after Muhammad Al-Khwarizmi, Tashkent, Uzbekistan*
[3] *PhD Doctor of Sciences Tashkent University of Information Technologies Named after Muhammad Al-Khwarizmi, Tashkent, Uzbekistan*
[4] *Assistant Tashkent University of Information Technologies Named after Muhammad Al-Khwarizmi, Tashkent, Uzbekistan*
**Corresponding author E-mail: omon_shoira@mail.ru*

Abstract

The article deals with the numerical solution of the problem of spatially loaded rods in linear and geometrically nonlinear statements. The results are presented in the form of graphs. A description of the results obtained and a comparative analysis of all parameters of the task set are given. A comparative analysis between linear and non-linear results is conducted. The aim of problem investigated the statics and dynamics of linear and geometrically nonlinear problem of stress-strain state of rods under spatial loading and the objects of problem are strained processes in linear and geometrically nonlinear problem of the statics and dynamics of rods under spatial loading are given.

Keywords: *Geometrical Nonlinearity; Oscillation; Rod; Spatial Load; Twisting.*

1. Introduction

Scientific research conducted in the world is aimed at constructing mathematical models, developing computational algorithms for solving linear and geometrically nonlinear problems of stress-strain state of rods under spatial loading, creating an automated system for estimating strain processes in rods. In this direction, the most important tasks are: construction of mathematical models that determine the stress-strain state, development of computational algorithms and creation of automated systems for estimating the strain processes of longitudinal-flexural, longitudinal-torsional and flexural-torsional oscillations of the rods under spatial loading. In this connection, the development of mathematical models and algorithms for solving problems of linear and geometrically nonlinear rods of complex configuration under spatial loading is urgent.

2. Statement of the problem

Mathematical models and computational algorithm for spatially loaded rods in linear and geometrically nonlinear statements are given in [2–11] with the following hypothesis:

$$\left.\begin{aligned} u_1(x,y,z,t) &= u(x,t) - \\ &\quad z\alpha_1(x,t) - y\alpha_2(x,t), \\ u_2(x,y,z,t) &= v(x,t) + z\theta(x,t), \\ u_3(x,y,z,t) &= w(x,t) - y\theta(x,t). \end{aligned}\right\}$$

where u_1, u_2, u_3 – the components of displacement vectors, x,y,z–spatial variables, θ – is an angle of torsion, u, v, w – displacements of a middle line of the rod, α_1, α_2 – the angles of sections rotation under pure bending, φ(y,z) – Saint-Venant function of torsion, defined from [1]:

$$\nabla^2\varphi = 0, \qquad \partial\varphi/\partial n = ly - mz.$$

On the basis of the Hamilton-Ostrogradsky's variation principle, of mathematical model was developed spatially loaded rods [2] – [5].

3. Mathematical model of spatially loaded rods

Here we present the systems of differential equations with the corresponding initial and boundary conditions [2], [9].
Fluctuations equations of spatially loaded rods.

$$-\rho F\frac{\partial^2 u}{\partial t^2} + \rho S_y\frac{\partial^2\alpha_1}{\partial t^2} + \rho S_z\frac{\partial^2\alpha_2}{\partial t^2} + \frac{\partial N_x}{\partial x} + \frac{\partial R_1}{\partial x} + \left(\bar{F}_1 + \bar{q}_1\right) = 0,$$

$$-\rho F\frac{\partial^2 v}{\partial t^2} - \rho S_y\frac{\partial^2\theta}{\partial t^2} + \frac{\partial Q_2}{\partial x} + \frac{\partial R_2}{\partial x} + \left(\bar{F}_2 + \bar{q}_2\right) = 0,$$

$$-\rho F\frac{\partial^2 w}{\partial t^2} + \rho S_z\frac{\partial^2\theta}{\partial t^2} + \frac{\partial Q_3}{\partial x} + \frac{\partial R_3}{\partial x} + \left(\bar{F}_3 + \bar{q}_3\right) = 0,$$

$$\rho S_y\frac{\partial^2 u}{\partial t^2} - \rho I_y\frac{\partial^2\alpha_1}{\partial t^2} - \rho I_{yz}\frac{\partial^2\alpha_2}{\partial t^2} + \frac{\partial M_y}{\partial x} + \frac{\partial R_4}{\partial x} - \left(M_y\left(\bar{F}_1\right) + M_y\left(\bar{q}_1\right)\right) = 0,$$

$$\rho S_z\frac{\partial u}{\partial t} - \rho I_{yz}\frac{\partial\alpha_1}{\partial t} - \rho I_z\frac{\partial\alpha_2}{\partial t} + \frac{\partial M_z}{\partial x} + \frac{\partial R_5}{\partial x} - \left(M_z\left(\bar{F}_1\right) + M_z\left(\bar{q}_1\right)\right) = 0,$$

$$-\rho S_y \frac{\partial^2 v}{\partial t^2} + \rho S_z \frac{\partial^2 w}{\partial t^2} + \rho I_\rho \frac{\partial^2 \theta}{\partial t^2} + \frac{\partial M_x}{\partial x} + \frac{\partial R_6}{\partial x} + \left(M_x\left(F_{23}\right) + M_x\left(q_{23}\right)\right) = 0.$$

Initial conditions:

$$\left[\rho F \frac{\partial u}{\partial t} - \rho S_y \frac{\partial \alpha_1}{\partial t} - \rho S_z \frac{\partial \alpha_2}{\partial t}\right]\delta u\Big|_t = 0,$$

$$\left[-\rho S_y \frac{\partial u}{\partial t} + \rho I_y \frac{\partial \alpha_1}{\partial t} + \rho I_{yz} \frac{\partial \alpha_2}{\partial t}\right]\delta\alpha_1\Big|_t = 0,$$

$$\left[-\rho S_z \frac{\partial u}{\partial t} + \rho I_{yz} \frac{\partial \alpha_1}{\partial t} + \rho I_z \frac{\partial \alpha_2}{\partial t}\right]\delta\alpha_2\Big|_t = 0,$$

$$\left[\rho F \frac{\partial v}{\partial t} + \rho S_y \frac{\partial \theta}{\partial t}\right]\delta v\Big|_t = 0, \quad \left[\rho F \frac{\partial w}{\partial t} - \rho S_z \frac{\partial \theta}{\partial t}\right]\delta w\Big|_t = 0,$$

$$\left[\rho S_y \frac{\partial v}{\partial t} - \rho S_z \frac{\partial w}{\partial t} + \rho I_\rho \frac{\partial \theta}{\partial t}\right]\delta\theta\Big|_t = 0.$$

Boundary conditions:

$$\left[-N_x + R_1 + \bar{\varphi}_1\right]\delta u\Big|_x = 0, \quad \left[-Q_2 + R_2 + \bar{\varphi}_2\right]\delta v\Big|_x = 0,$$

$$\left[-Q_3 + R_3 + \bar{\varphi}_3\right]\delta w\Big|_x = 0, \quad \left[-M_y + R_4 + M_y\left(\varphi_1\right)\right]\delta\alpha_1\Big|_x = 0,$$

$$\left[-M_z + R_5 + M_z\left(\varphi_1\right)\right]\delta\alpha_2\Big|_x = 0, \quad \left[-M_x + R_6 + M_x\left(\varphi_{23}\right)\right]\delta\theta\Big|_x = 0.$$

where F - cross sectional area, S_y, S_z - static moments, I_y, I_z - the axial or equatorial moments of inertia of the area relative to the x and y axes, I_{yz} - centrifugal moment of inertia is relatively x and y axes, I_ρ - polar moment, M_y, M_z - shear moments, N_x - the longitudinal squeezing loading, Q_2, Q_3 - shear forces, M_x - twisting, $R_1, R_2, R_3, R_4, R_5, R_6$ - nonlinear parameters, $\bar{F}_1, \bar{F}_2, \bar{F}_3$ - bulk forces, $\bar{q}_1, \bar{q}_2, \bar{q}_3$ - surface forces and their forms are given in [8], [10].

4. Numerical solution of spatially loaded rods

Here, as an example, consider a rod with fixed ends and longitudinal force q_1, transverse forces q_2, q_3 and moment M.

The following values of parameters are used for calculations of the rods: Young's modulus $E = 2 \cdot 10^5\ Pa$, Poisson's ratio $\nu_1 = 0,3$ (for steel), length $l = 10\ m$, cross-section dimensions $a = 0,02\ m$, $b = 0,02\ m$, surface loads $q_1 = 0,015$ H, $q_2 = 0,01$H, $q_3 = 0,02$H, $M = 0,012\text{H} \cdot m$.

Figs. 1 - 6 show longitudinal, transverse and torsion oscillations with the functions of longitudinal displacement $u(x,t)$, transverse displacements $v(x,t), w(x,t)$, angles of inclination $\alpha_1(x,t), \alpha_2(x,t)$ and torsion angle $\theta(x,t)$ for a rod, the two ends of which are rigidly fixed. The results are obtained for linear and non-linear statements at different moments of time.

Fig. 1 shows the graphs of propagation of longitudinal oscillations $u(x,t)$ along the length of the rod l=10 m at the moments of time t = 40 s and 80 s.

Fig. 1 shows the graphs of results of longitudinal displacement u along the length of the rod at different moments of time t = 40 s and t = 80 s. As seen from the graphs at different moments of t along the length of the rod there are different results at different points: increasing sinusoidal amplitudes appear closer to the points of the center of the rod.

From Fig. 1 it is seen that longitudinal displacement u has the greatest disturbance in the middle of the rod. Further, the displacement values are reduced at the ends of the rod. At t = 40 s, longitudinal displacement u has small value, it gradually increases and at t = 80 s has the greatest value.

As seen from Fig. 1, longitudinal displacement $u(x,t)$ has the greatest disturbance in the middle of the rod. When moving to the ends of the rod, the disturbances attenuate. With increasing time, the amplitude of oscillations increases. The symmetry of oscillations of the relative middle cross section is observed. Here the number of iterations is k=9.

Fig. 2 shows the propagation of transverse oscillations v along the length of the rod for the boundary conditions of the rigid fixing at two ends in linear and non-linear statements at different moments of time. As seen from the figure for transverse oscillations v, the greatest disturbance appears at the ends of the rod, it gradually decreases in the middle of the rod. At t = 40 s transverse oscillation v has a small value, it gradually increases and at t = 80 s has the greatest value. With increasing time t, the transverse oscillation v at the end points of the rod takes on the greatest value and moves symmetrically to the maximum value relative to the center of the length of the rod.

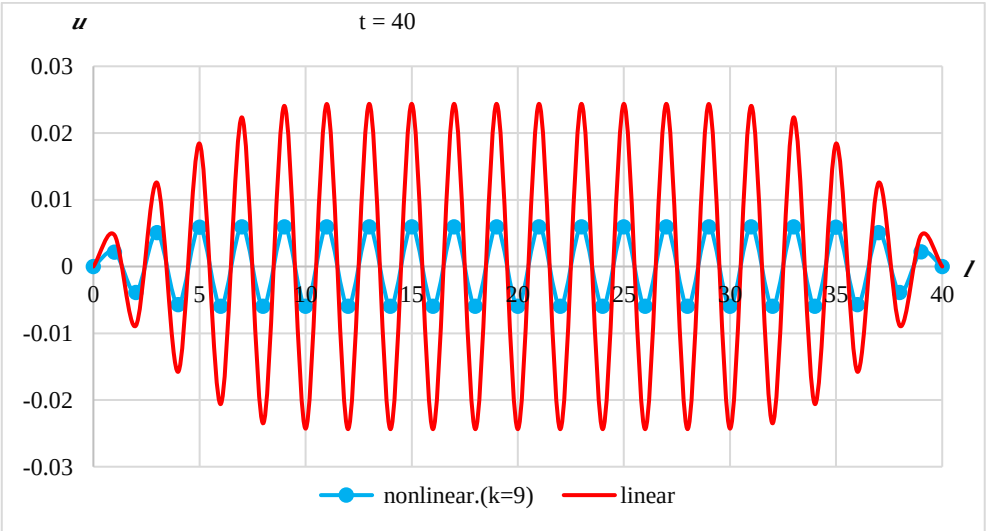

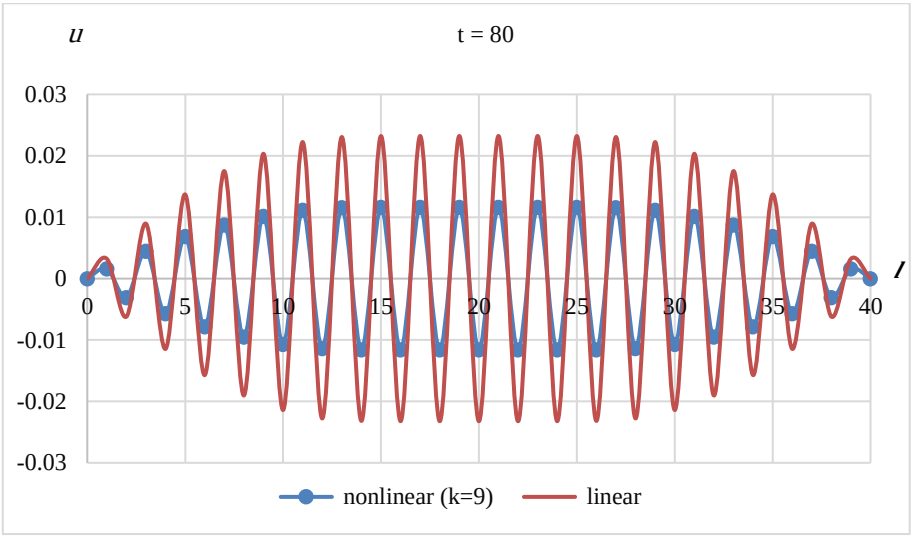

Fig. 1: Propagation of Longitudinal Vibrations $u \times 10^{6}$ along the Length of the Rod l=10 M at Different Moments of Time.

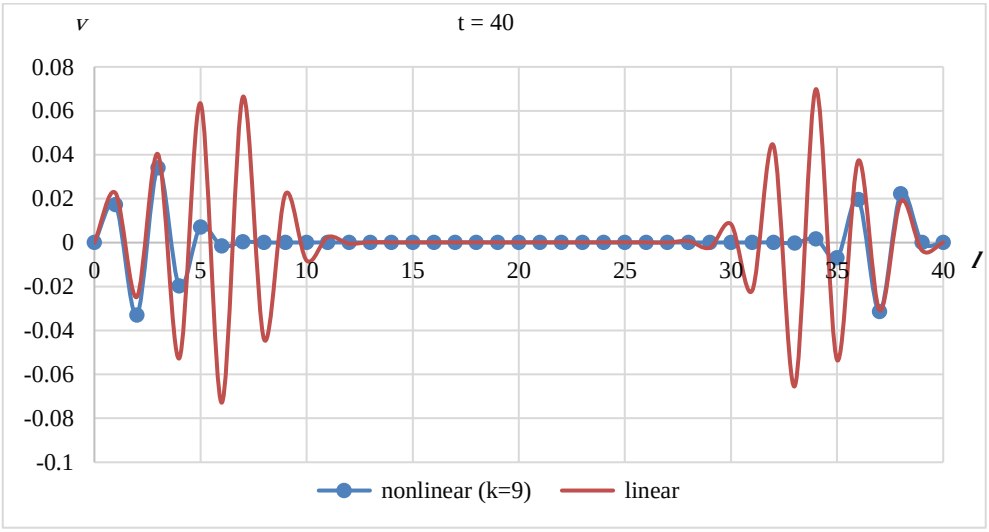

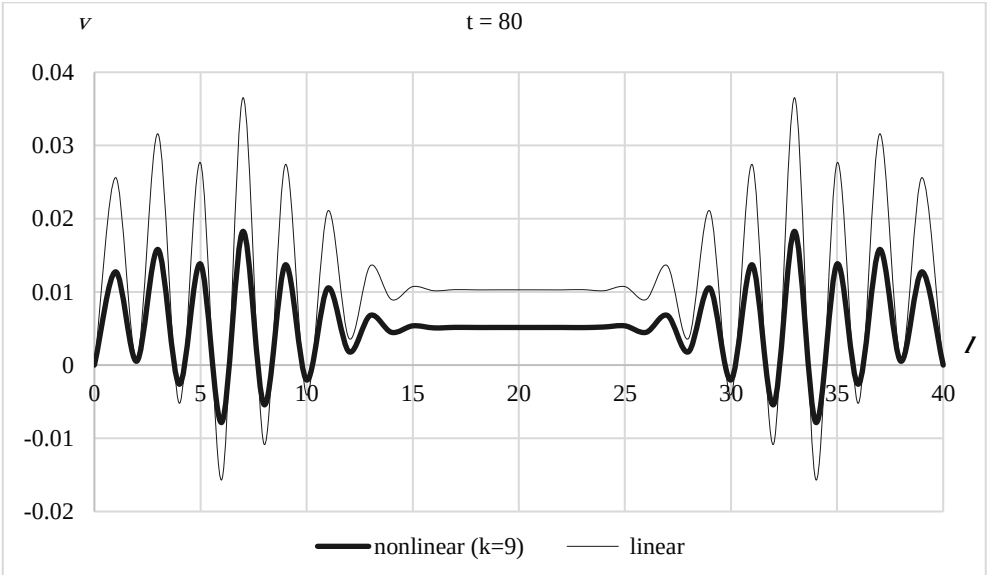

Fig. 2: Propagation of Transverse Oscillations $v \times 10^{4}$ along the Length of the Rod l = 10 M and at Moments of Time T = 40 S and 80 S.

Fig. Figure 3 shows the transverse oscillation w propagation along the rod for boundary conditions of the rigid fixing of two ends in linear and non-linear statement at moments of time $t = 40\,s$ and $80\,s$. As seen from the figure for transverse oscillation w the greatest disturbance is observed at the ends of the rod, it gradually decreases as it approaches the center of the rod. At t = 40 s, transverse oscillation w has small value, it gradually increases, and at t = 80 s it takes on the greatest value.

With increasing time t, transverse oscillation w at the end points of the rod takes on the greatest value and moves symmetrically to the maximum value relative to the center of the length of the rod. The value of transverse oscillations w corresponding to the greatest amplitude is observed at the initial time t and at t = 20 s near the points of the boundary, with increasing time t, for example, at t = 80 s, it is close to the center and has the greatest value.

It is established that transverse oscillations in the case of a nonlinear model have the less value of amplitude and the process is more stable. There is an increase in the frequency of oscillations in comparison with the linear case. This result is consistent with the research results on nonlinear dynamics of mechanisms and machines, while the analysis of displacements of elastic elements in nonlinear statement differs from the one in linear statement of the problem.

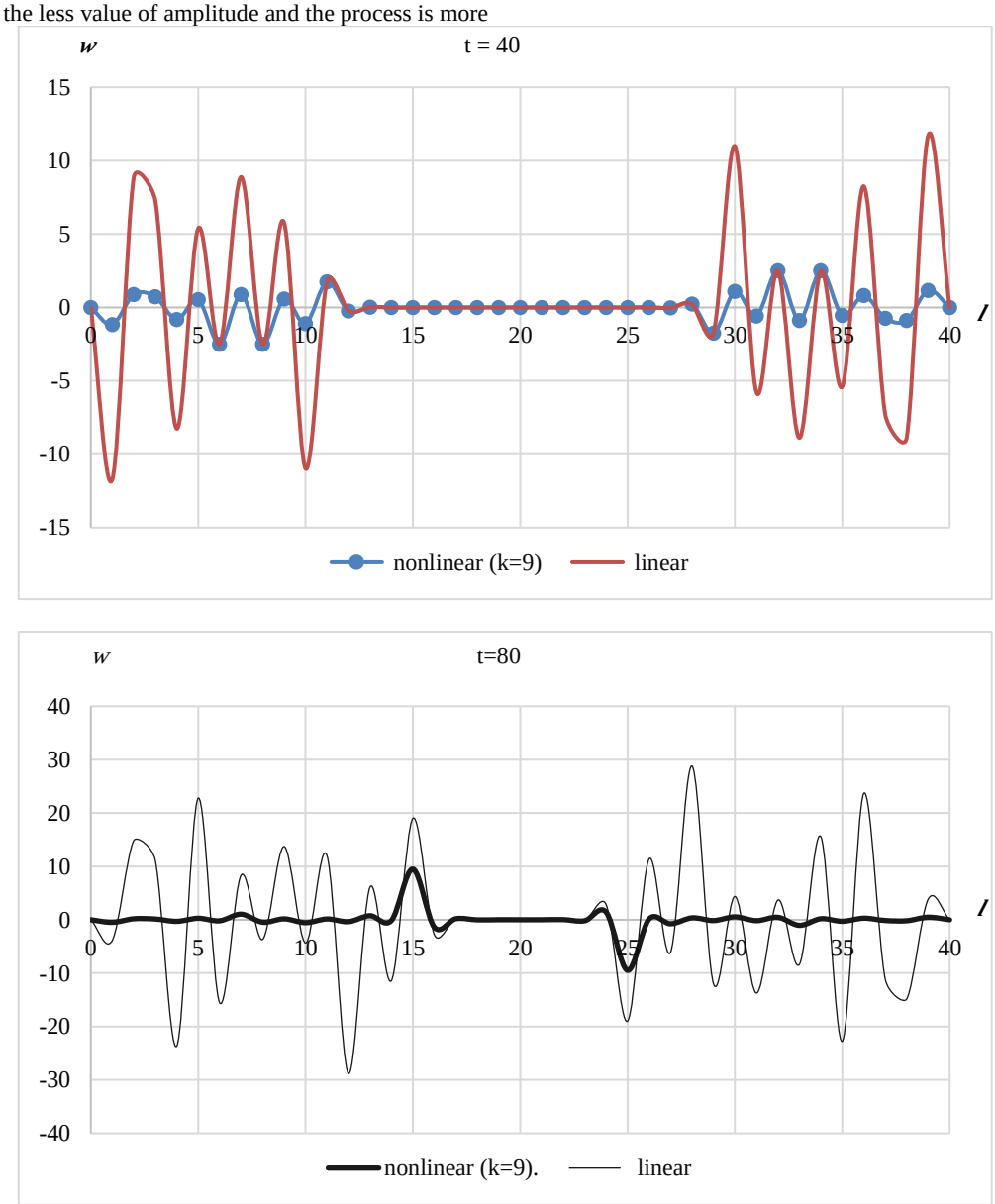

Fig. 3: Propagation of Transverse Oscillations $w \times 10^2$ along the Length of the Rod l = 10 M at Moments of Time T = 40 S and 80 S.

Fig. 4 shows the graphs of oscillation propagation of the angle of inclination α_1 along the length of the rod l = 10 m at moments of time t = 40 s and 80 s. The length of the rod is divided into eight fourth. According to these graphs, at t = 40 s the greatest disturbance of the angle of inclination α_1 appears at the ends of the rod, it gradually decreases in the middle of the rod. At the moment of time t = 80 s the angle of inclination α_1 at the ends of the rod has small value, the greatest disturbance of the angle of inclination α_1 appears at 2l/8, 3l/8, 6l/8 and 7l/8 quarter of the rod, and it decreases to the middle of the rod.

Fig. 5 shows the graphs of oscillation propagation of the angle of inclination α_2 along the length of the rod at different moments of time t = 40 s and 80 s. According to the graphs, the angle of inclination α_2 has the greatest disturbance at the ends of the rod and it gradually decreases towards the middle of the rod. At t = 40 s the angle of inclination α_2 is small, it gradually increases and at t = 80 s it takes on the greatest value. According to these graphs, with an increase in time at two rigidly fixed ends there is an increase in the oscillations toward the center of the rod and different values of the oscillations occur at different points of the rod. At t = 40 s, the oscillation amplitude is small and only at boundary points it takes on a non-zero value; at t = 80 s the amplitude of oscillations increases, the largest values are reached at 3l/8, 6l/8 and have negative values. At increasing time the angle of inclination α_2 is negative.

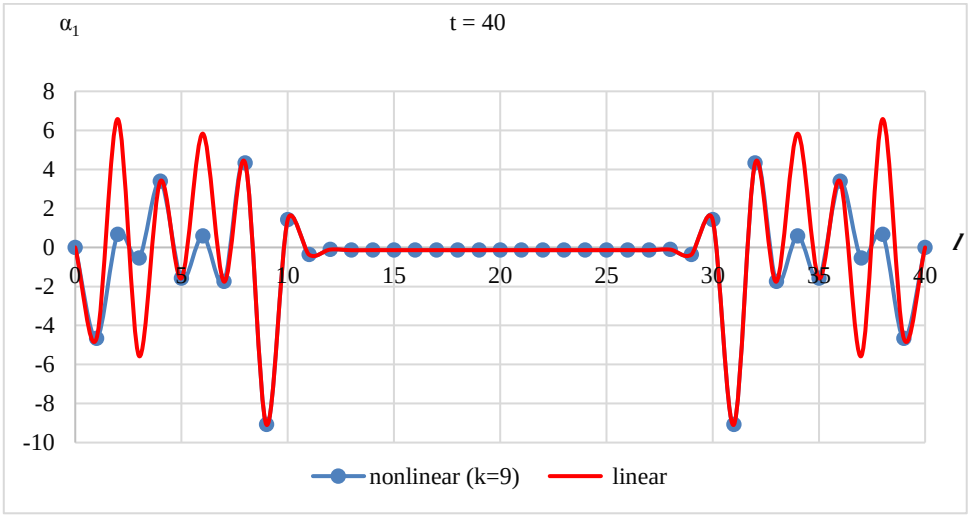

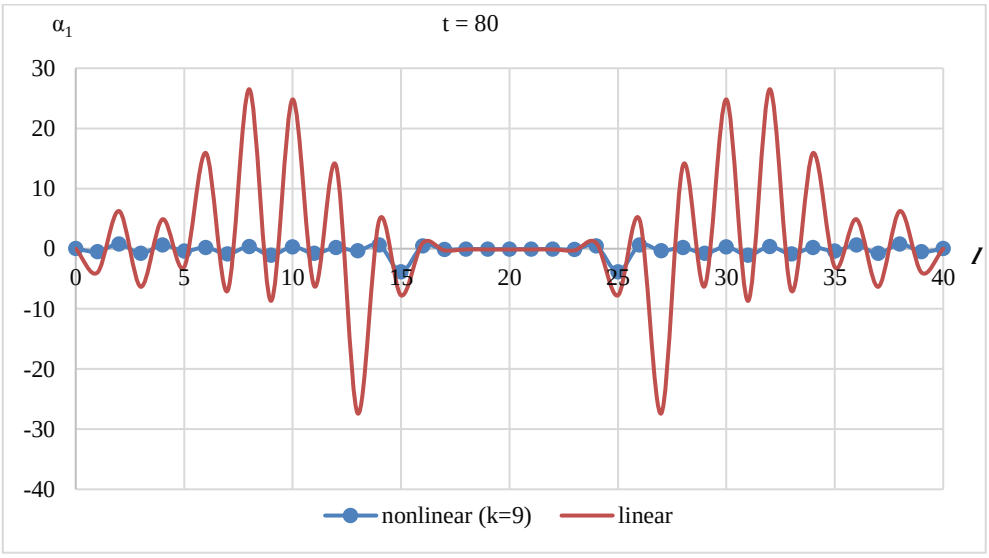

Fig. 4: Oscillation Propagation of the Angle of Inclination $\alpha_1 \times 10^5$ along the Length of the Rod at Different Moments of Time.

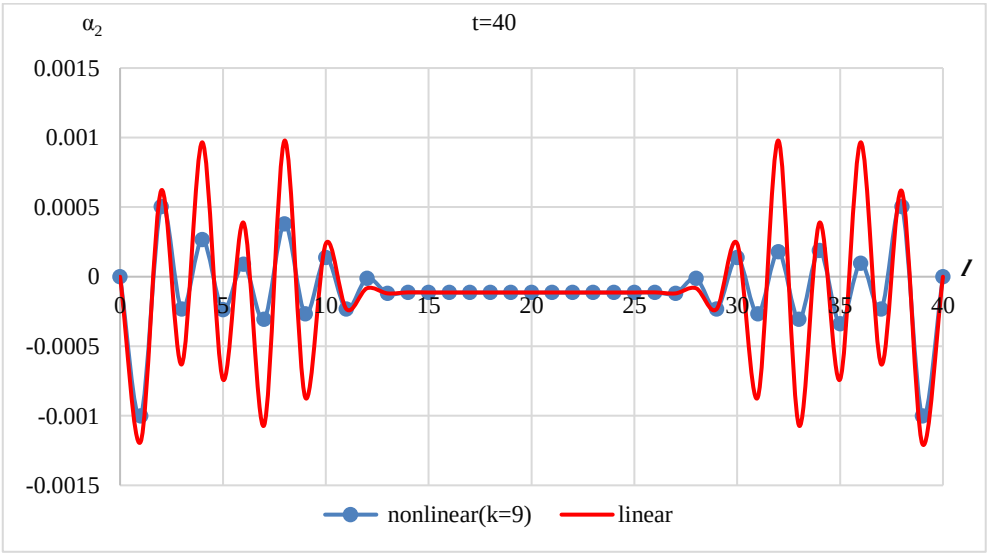

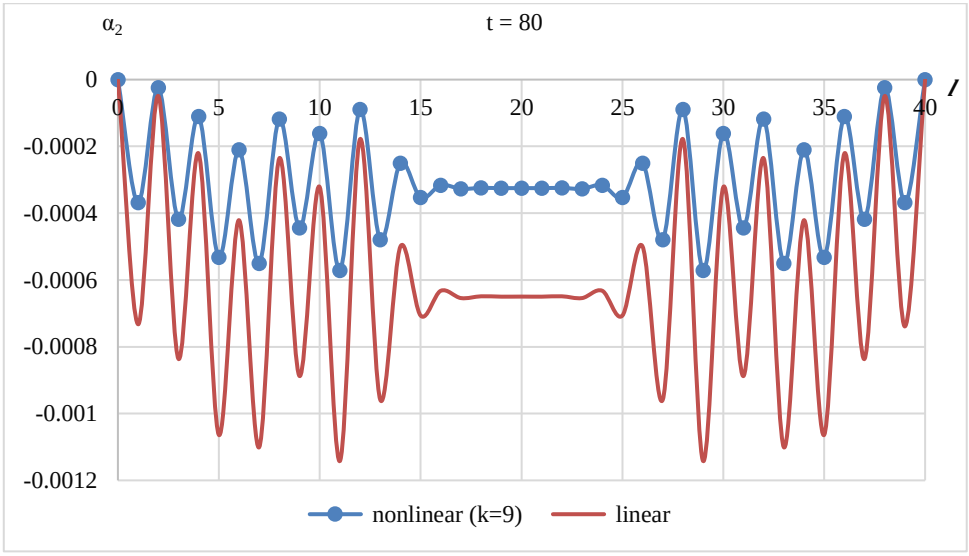

Fig. 5: Oscillation Propagation of the Angle of Inclination $\alpha_2 \times 10$ along the Length of the Rod at Moments of Time T = 40 S and T = 80 S.

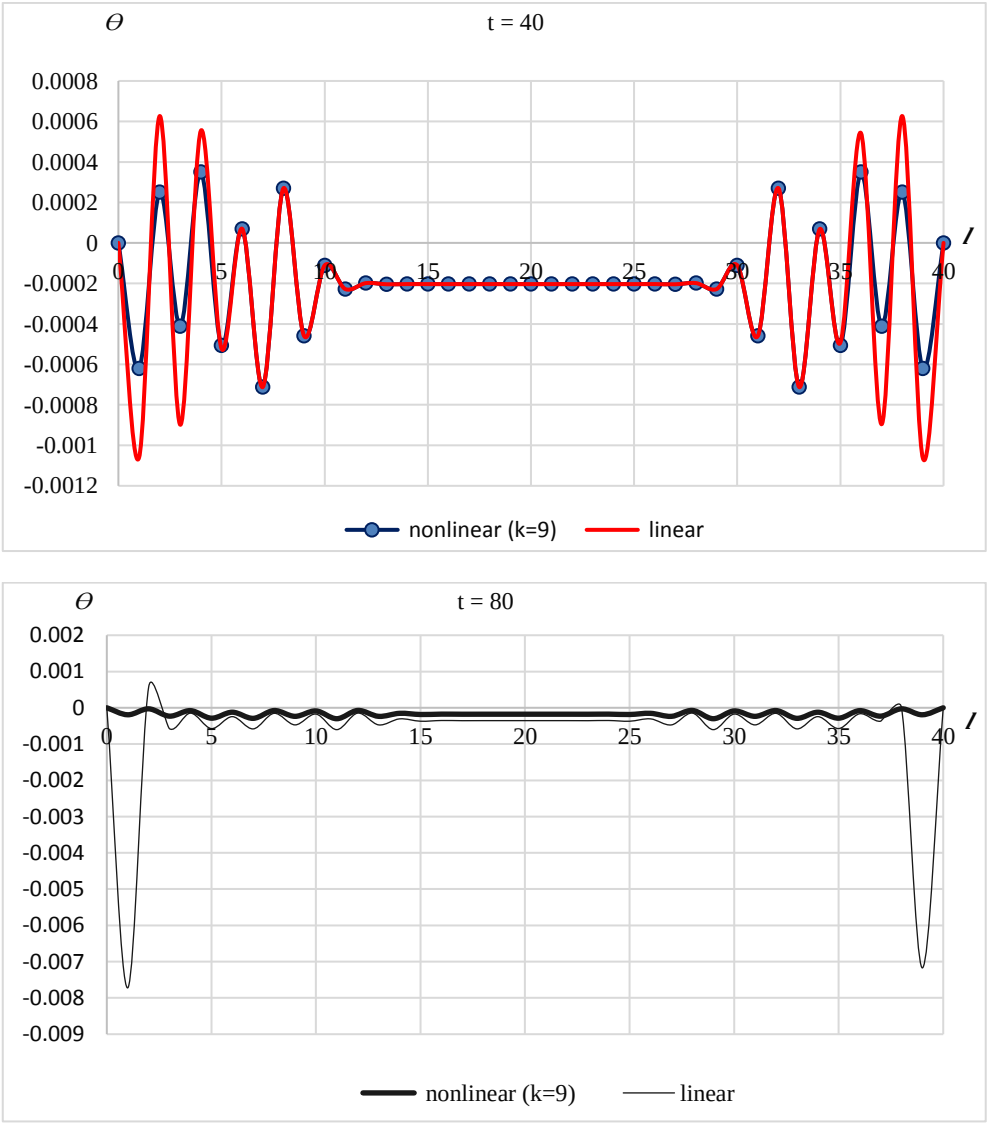

Fig. 6: Oscillation Propagation of the Angle of Torsion $\theta \cdot 10^3$ along the Length of the Rod at Different Moments of Time T.

In fig. 6 shows the graphs of oscillations propagation of the angle of torsion θ along the length of the rod at different moments of time t = 40 s and 80 s. From these graphs it follows that the angle of torsion θ has the greatest disturbance at the ends of the rod, and gradually decreases towards the middle of the rod. With increasing time, the value of disturbance gradually increases. For short values of time the main oscillations occur in the boundary region of the rod with fixed ends. In the middle part a constant value is set. With time the disturbances are transferred closer to the center and the middle part at t = 40 s and 80 s has a constant non-zero value. If the middle part of the constant torsion at t = 40 s has had a positive value, then with time it takes a negative value. This figure

shows the localization of large amplitudes closer to the ends of the rod. Here the number of iterations is k = 9.

5. Conclusions

The results obtained are consistent with the results of research carried out on nonlinear dynamics of rods, when the displacements of elastic elements in linear statement differ from the ones in nonlinear statement of the problem. This suggests that the rod structure studied here with geometric and physical parameters is essentially nonlinear. Therefore, linear modeling of this problem will lead to the first approximation of solutions. In addition, it will reflect the diversity of complex oscillatory processes that occur at multiple frequencies, which will remain outside the framework of linear dynamic models.

References

[1] V. K. Kabulov Algorithmization in elasticity theory and deformation theory of plasticity. Tashkent: Fan, 1966. -394 p.

[2] Sh. A. Anarova, T.Yuldashev. Mathematical Model of Nonlinear Equations of Rod Oscillations under Dynamic Loading, Uzbek Journal Problems of Informatics and Power Engineering, Tashkent (2014) № 6. - Pp. 36-42.

[3] Sh. A. Anarova, T. Yuldashev. Mathematical Models of Spatially Loaded Rods with Allowance for the Torsion Function and Transverse Shears, TATU Habarlari (2014) № 4 (32). - Pp. 76-86.

[4] Sh. A. Anarova, T. Yuldashev. Derivation of Mathematical Model of Spatially Loaded Rods with Allowance for the Torsion Function and Transverse Shears, Problems of Computational and Applied Mathematics. Tashkent, (2015) № 1. -Pp. 28-40.

[5] Sh. A. Anarova, F. M. Nuraliev, G. Dadenova. Mathematical Model of Spatially Loaded Rods with Torsion Function and Transverse Shears, International Journal of Technical Research and Applications, Volume 4, Issue 1 (January-February, 2016). - Pp. 22-32.

[6] Sh.A.Anarova, A.Sh.Nazirov. The Structure of the Complex of Programs for the Study of the Stress-strain State of Elastic Prismatic Bodies of Arbitrary Section, TATU Habarlari. (2016) № 1 (37). - Pp. 51-59.

[7] Sh. A. Anarova, Sh. Sh. Safarov. Software for Stress-strain State of Rods under Static Loading, Problems of computational and applied mathematics. Tashkent (2016). № 4. - Pp. 20-34.

[8] Sh. A. Anarova, N. G. Eshkaraeva. Processes for Solving a Geometrically Nonlinear Problem of Rods with Arbitrary Mechanical and Geometrical Characteristics, Proc. of Republican Scientific-technical Conference. September 8-9, (2017). - Samarkand, – Pp. 36-42.

[9] Sh.A. Anarova Algorithm of Solution of Geometrically Nonlinear Problem of Rods with Arbitrary Mechanical Geometrical Characteristics, International Journal of Advanced Research in Science, Engineering and Technology IJARSET.com Volume 4, Issue 11 (November, 2017). - Pp. 4796-4815.

[10] Sh. A. Anarova. Numerical Simulation of Rod Oscillations, Problems of Computational and Applied Mathematics. Tashkent, (2017). № 5. - Pp. 4-10.

[11] Sh. A. Anarova, T. Yuldashev. Derivation of Differential Equations of Oscillation of Rods in Geometrically Nonlinear Statement, Problems of Computational and Applied Mathematics. Tashkent, (2018). № 2. - Pp. 72-105.